AD-A093 159 GEORGIA INST OF TECH ATLANTA FRACTURE AND FATIGUE RE--ETC F/G 11/6
THE EFFECT OF OVERLOAD ON FATIGUE CRACK PROPAGATION IN METASTAB--ETC(U)
NOV 80 E W LEE, S B CHAKRABORTTY N00014-75-C-0349
UNCLASSIFIED GIT-TR-80-1 NL

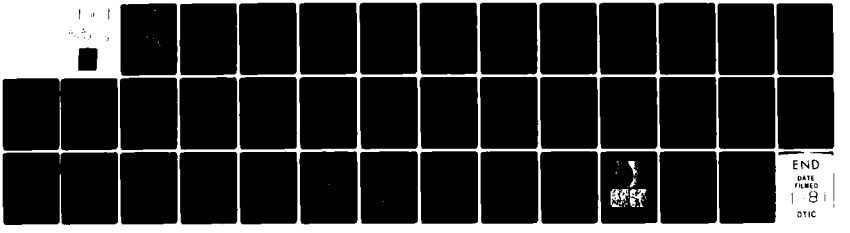

END
DATE FILMED
1-81
DTIC

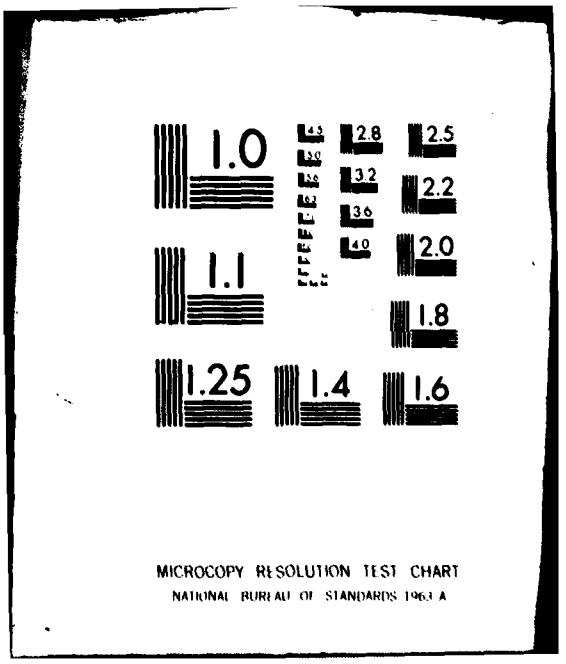
1.0
1.1
1.25
1.4
1.6
1.8
2.0
2.2
2.5
2.8
3.2
3.6
4.0
MICROCOPY RESOLUTION TEST CHART
NATIONAL BUREAU OF STANDARDS 1963 A

SECURITY CLASSIFICATION OF THIS PAGE (When Data Entered)

REPORT DOCUMENTATION PAGE

READ INSTRUCTIONS BEFORE COMPLETING FORM

1. REPORT NUMBER	2. GOVT ACCESSION NO. AD-A093159 / 3. RECIPIENT'S CATALOG NUMBER
4. TITLE (and Subtitle) THE EFFECT OF OVERLOAD ON FATIGUE CRACK PROPAGATION IN METASTABLE BETA TITANIUM-VANADIUM ALLOYS	5. TYPE OF REPORT & PERIOD COVERED Technical Report 80-1 / 6. PERFORMING ORG. REPORT NUMBER
7. AUTHOR(s) Eui-Whee Lee and Saghana B. Chakrabortty	8. CONTRACT OR GRANT NUMBER(s) N00014-75-C-0349
9. PERFORMING ORGANIZATION NAME AND ADDRESS Fracture and Fatigue Research Laboratory Georgia Institute of Technology Atlanta, Georgia 30332	10. PROGRAM ELEMENT, PROJECT, TASK AREA & WORK UNIT NUMBERS
11. CONTROLLING OFFICE NAME AND ADDRESS Metallurgy Program, Material Sciences Div. Office of Naval Research 800 N. Quincy St., Arlington, VA 22217	12. REPORT DATE November 28, 1980 / 13. NUMBER OF PAGES 35
14. MONITORING AGENCY NAME & ADDRESS (if different from Controlling Office)	15. SECURITY CLASS. (of this report) Unclassified / 15a. DECLASSIFICATION/DOWNGRADING SCHEDULE

LEVEL II

16. DISTRIBUTION STATEMENT (of this Report)

Unlimited

DTIC ELECTE DEC 18 1980 S C

17. DISTRIBUTION STATEMENT (of the abstract entered in Block 20, if different from Report)

18. SUPPLEMENTARY NOTES

19. KEY WORDS (Continue on reverse side if necessary and identify by block number)

Fatigue Crack Propagation, Overload Effects, Fatigue Crack Retardation, Delay Cycles, Metallurgical Factors, Single Cycle Overload, Multiple Cycle Overload, Overload Ratio, Stress Ratio, Fractographic Features, Deformation Modes.

20. ABSTRACT (Continue on reverse side if necessary and identify by block number)

The crack retardation response due to single- and multiple-cycle overload of two titanium vanadium alloys (24 and 32 wt. pct. V) has been studied. It has been observed that the degree of retardation depends upon the vanadium content of the alloy, the load ratio, the number of overload cycles and the magnitude of the peak load. Fractographic observations show that the cracking mode may be changed in the overload affected zone from that in the pre-overload region. These results seem to indicate that the retarda-

DD FORM 1 JAN 73 1473

SECURITY CLASSIFICATION OF THIS PAGE (When Data Entered)

20. Abstract (Continued)

tion behavior is mainly due to the compressive residual stresses arising as a consequence of the overload. The degree of retardation depends not only on the loading variables, but also on the material parameters like the monotonic and cyclic deformation behavior, and the stress-strain response.

(14) GIT-TR-80-1

OFFICE OF NAVAL RESEARCH

(15) Contract N00014-75-C-0349, NR 031-75

(12) 39

(9) TECHNICAL REPORT, 80-1

(6) # THE EFFECT OF OVERLOAD ON FATIGUE CRACK PROPAGATION IN METASTABLE BETA TITANIUM-VANADIUM ALLOYS.

By

(10) Eui Whee Lee and Saghana B. Chakrabortty

November 28, 1980

(11) 28 Nov 80

FRACTURE AND FATIGUE RESEARCH LABORATORY
GEORGIA INSTITUTE OF TECHNOLOGY
ATLANTA, GEORGIA 30332

THE EFFECT OF OVERLOAD ON FATIGUE CRACK PROPAGATION IN METASTABLE BETA TITANIUM-VANADIUM ALLOYS

E. W. Lee and S. B. Chakrabortty
Fracture and Fatigue Research Laboratory
Georgia Institute of Technology
Atlanta, Georgia 30332

ABSTRACT

The crack retardation response due to single- and multiple-cycle overload of two titanium vanadium alloys (24 and 32 wt. pct. V) has been studied. It has been observed that the degree of retardation depends upon the vanadium content of the alloy, the load ratio, the number of overload cycles and the magnitude of the peak load. Fractographic observations show that the cracking mode may be changed in the overload affected zone from that in the preoverload region. These results seem to indicate that the retardation behavior is mainly due to the compressive residual stresses arising as a consequence of the overload. The degree of retardation depends not only on the loading variables, but also on the material parameters like the monotonic and cyclic deformation behavior, and the stress-strain response.

INTRODUCTION

Recent studies have shown that application of overload during fatigue crack propagation leads to a retardation in crack growth in the overload affected zone ahead of the crack-tip[1-15]. The degree of crack retardation depends upon the loading variables like the stress intensity range, extent of overload, number of overload cycles, load ratio, frequency of loading, specimen thickness (plane strain or plane stress), etc. Material parameters like yield strength[5,6], strain hardening exponent [9,13-15], fracture toughness[12], etc., also have been found to have an influence. This research was undertaken to observe the influence of materials' deformation behavior on the overload response of two metastable beta titanium-vanadium alloys and to elucidate the mechanisms involved.

Previous workers[16-24] have shown that deformation modes, microstructure, low cycle fatigue (LCF) and fatigue crack propation (FCP) properties of titanium-vanadium alloys may be varied substantially by varying vanadium content and aging time and temperature. The two alloys chosen for this work are Ti-24%V and Ti-32%V. In the as quenched condition the deformation behavior changes from coarse twinning and fine wavy slip for the 24% alloy to coarse planar slip for the 32%V alloy. The 32%V alloy has a higher yield stress, a lower degree of cyclic hardening and a better cyclic strain-life response when compared to the 24%V slloy. The fatigue crack growth rate (FCGR) in air of the 32%V alloy is lower in the low stress intensity range (ΔK) and higher in the intermediate ΔK. The mechanism of

fatigue crack growth appears to be similar for both alloys. At low growth rates ($da/dn < \sim 10^{-8}$ m/cycle) the fracture surface appears to have ill defined cleavage facets which are usually considerably smaller than the grain size (multifaceted growth). At intermediate growth rates ($\sim 10^{-8}$ m/cycle $< \sim 2.5 \times 10^{-7}$ m/cycle), the fracture surface is composed of large facets each of which usually covers one whole grain (faceted growth). At high growth rates ($da/dn > \sim 2.5 \times 10^{-7}$ m/cycle), the fracture surface is more or less flat, is perpendicular to the stress axis and is composed of fatigue striations and microvoids (non-crystallographic growth).

The two alloys chosen for our studies have differences in monotonic and cyclic stress-strain response and deformation behavior. They have similar fatigue crack growth characteristics with distinct fractographic features. These considerations make these alloys suitable for studying the influence of the metallurgical factors on the overload effects on fatigue crack propagation.

EXPERIMENTAL

Two Ti-V alloys containing 24 and 32 wt. pct. vanadium were prepared by Titanium Metals Corporation (Henderson, Nevada), where 14cm diameter ingots were hot forged and hot rolled to produce 150 x 150 x 8 mm plates having a random texture. The chemical analysis and grain intercept length of these materials are shown in Table I. Samples from the as received plates were solutionized at 780°C for two hours in dry argon and quenched in iced water. Compact tension[25] samples with H/W of 0.486, W = 44.5mm, and B = 6.4mm were used for FCP tests. The starter

notches were machined after heat treatment. FCP tests were performed on a servohydraulic closed loop MTS testing machine using tension-tension sinusoidal loading. Crack lengths were measured within 0.01 mm on the polished surface of the specimen using a Gaertner travelling microscope. The tests were carried out in laboratory air with a relative humidity of $\sim$ 30pct. and at a temperature of $\sim$ 25^{o}C.

Figure 1 is schematic of a typical load program for the overload experiments. Crack growth at the base stress intensity range before (region A, Figure 1) or after (region C, Figure 1) the application of overload was conducted at 10 Hz. The application of one cycle overload was done at 0.2 Hz and 100 cycle overload at 1 Hz (region B, Figure 1). The fracture surfaces were examined with optical and scanning electron microscopy.

RESULTS

General Crack Arrest Behavior: The basic data obtained during the tests are crack length and the number of applied cycles. Crack length as a function of cycles near the overload region is shown in Figure 2. The slope represents crack growth rate. The arrows indicate the starting point for the application of overload. The slope prior to the application of overload represents the normal crack growth rate at the base stress intensity range (ΔK_b). The sharp increase in this slope is due to the application of the overload. The horizontal line represents the complete arrest of crack growth after overload.

Complete arrest behavior has been reported previously by other investigators[1,7]. However, it is argued that the crack may propagate so slowly in the region that it is undetectable by the ordinary crack length measuring technique. The delay period N_d is taken from the point where the overload was applied to the point where the crack growth rate returned to its original value at that stress amplitude[5]. The total number of cycles of reduced crack growth rate is usually less than one tenth of the total number of arrest cycles.

Figure 3 illustrates the crack propagation rate as a function of distance from the overload region at different base line stress intensity ranges. Initially the crack growth rate decreases sharply and later increases as the distance from the overload region increases. As shown in this figure, this effect is significant for higher ΔK_b.

Effect of Number of Overload Cycles on Retardation: Figure 4 shows the number of delay cycles as a function of base line stress intensity for the 100 percent overload experiments. Delay cycles times the crack growth rate during nonoverload condition as a function of ΔK_b is shown in Figure 5. The value of $da/dN \times N_d$ is the actual crack length difference between the overload condition and the nonoverload condition.

The results shown in Figures 4 and 5 may be summarized by the following:

1. Retardation decreases as the base line stress intensity range increases regardless of the number of overload cycles and vanadium content.

2. The one hundred cycle overload produces a larger number of delay cycles than the one cycle overload for both alloys.
3. The retardation difference between the 100-cycle overload and the one cycle overload is greater for the Ti-24V alloy than for Ti-32V alloy.
4. The Ti-24V alloy shows a larger retardation than the Ti-32V alloy in the low stress intensity range. The reverse is true in the high stress intensity range.
5. The retardation difference between the 100-cycle overload and one cycle overload decreases as the stress intensity increases.
6. N_d x da/dN is larger for the 100-cycle overload than for the one cycle overload. For the one cycle overload, it increases as ΔK_b increases. For the 100-cycle overload, it decreases as ΔK_b increases.
7. N_d x da/dN for the one cycle and 100-cycle overload converges as ΔK_b increases in both cases.
8. When compared with the Ti-32V alloy, the Ti-24V alloy has a larger N_d x da/dN in the lower ΔK_b range and smaller values in the higher ΔK_b range.

Effects of Overload Ratio on Retardation: N_d versus ΔK_b curves for 100 cycle overload at 50 percent and 100 percent overload ratios are illustrated in Figure 6. Fifty percent overload results in a far smaller number of delay cycles than the 100 percent overload. For 50% overload minor differences between the Ti-24V and Ti-32V alloys are observed. Figure 7 compares the

N_d x da/dN versus ΔK_b curves for 100 cycle overload at 50 pct. and 100 pct. overload ratios.

The effect of a two hundred percent overload on the Ti-32V alloy was determined for the base line stress intensity range of 20 MPa$\sqrt{m}$. For one cycle overload, 200 percent overload produces approximately 15 times larger N_d than 100 percent overload, Figure 8. For 100 cycle overload, 100 times larger N_d was observed for 200 percent overload than for 100 percent overload. Comparing the results for 50, 100 and 200 pct. overload for a given ΔK_b, N_d appears to increase exponentially as the overload ratio increases at this stress level, Figure 8.

Effects of Stress Ratio on Retardation: Effects of overload at different stress ratio were investigated for the Ti-32V alloy. The load program and results of these studies are shown in Figure 9 and Table III. The important features of this test are described as follows:

1. If the overload ratio is kept constant, N_d decreases with increasing R ratio. However, when the R ratio is above 0.5, the decrease in N_d is negligible (Table IIIa).
2. For the higher R ratio, the difference of N_d between one cycle overload and 100 cycle overload is smaller than for the lower R ratio (Table IIIb).
3. N_d depends largely upon K_{OL} regardless of K'_{min} of overload cycles. For example, when ΔK_b and K_{OL} are 8 MPa$\sqrt{m}$ and 16 MPa$\sqrt{m}$ respectively, N_d is 10^6 cycles regardless of whether K'_{min} is 0.8 or 8 MPa$\sqrt{m}$ (Table IIIc).

Comparison with Previous Results: The results of the overload experiments on the Ti-V alloys agree with results presented by others[1-9] with respect to some general features and they may be summarized as follows:

1. The retardation effect (N_d) increases as the overload ratio increases up to a certain level[3,4,8,9].
2. The retardation effect (N_d) increases as the number of cycles of applied overload increases[2,4,8,9].
3. The retardation effect (N_d) decreases as the base line stress intensity increases[1,3,5,6].

Fractographic Features: Figure 10 shows the features of the fracture surfaces before, during and after the application of 100 pct. overload for the Ti-24V alloy for a base stress intensity range of 30 MPa$\sqrt{m}$. SEM fractographs in Figures 10b and 10c show the features of the pre and post overload regions in some details. Substantial differences in fracture morphologies can be observed even though the applied stress intensity range in these two regions are the same. For the preoverload region (Figure 10b) the fracture surface is flat and featureless at low magnifications and shows ductile striations and microvoids at higher magnifications. This agrees with the results of Chakrabortty and Starke[17] who also have observed these non-crystallographic features in the Ti-24V alloy fatigued at a high stress intensity range like 30 MPa$\sqrt{m}$. In contrast, the fracture surfaces at the immediate post overload region show facet features even though the applied stress intensity range

is again approximately 30 MPa$\sqrt{m}$. Chakrabortty and Starke[17] have shown that for the Ti-24V alloy, this faceted growth occurs at the stress intensity range values of approximately 9 to 20 MPa$\sqrt{m}$. This probably indicates that the effective stress intensity in the immediate post overload region is below 20 MPa$\sqrt{m}$ even though the applied stress intensity range is 30 MPa$\sqrt{m}$. That is, a substantial reduction in the effective stress intensity range may occur immediately after the application of overload.

DISCUSSION

The explanations offered for delay effects observed after overloading make use of mechanisms which may be broadly divided into five categories[3], which are: (i) residual compressive stresses at or near the crack tip[26], (ii) closure effects generated by the crack tip deformation[27], (iii) crack tip blunting[28], (iv) crack tip strain hardening[1] and (v) crack tip branching[29]. All these effects may arise chiefly due to the greater plastic deformation at or near the crack tip during the application of overload. The delay behavior of the titanium-vanadium alloys used in our studies may be explained in terms of the residual stress and crack closure arguments. The number of delay cycles seem to depend on the magnitude of the residual stresses and the interaction of these stresses with the subsequently applied base line cyclic stresses. With this argument we shall discuss our result in the remainder of this section.

General Crack Arrest Behavior: The observed crack arrest cycles and the subsequent growth behavior shown in Figure 3 may be explained with the schematic diagram shown in Figure 11. Application of the overload produces a large overload plastic zone (region A in Figure 11) in front of the crack tip. A portion of this zone immediately ahead of the crack tip will be under residual compressive stresses once the overload is withdrawn. These residual stresses will counteract the subsequently applied stresses and the crack does not grow for a number of cycles. The application of cyclic stresses, however, releases the residual stresses and forms a small plastic zone (region B in Figure 11) in front of the crack tip and within the overload plastic zone. After a critical number of cycles (cycles of crack arrest), the crack starts to grow because the residual stress in front of the crack tip is sufficiently released. Initially, the crack growth rate is relatively high. But the growth rate decreases sharply because the effect of the release in residual stress by the crack arrest cycles decreases as the crack tip moves away from point O (Figure 11). As the crack tip advances much further, the residual stress becomes less and as a consequence, the crack growth rate increases sharply and returns to its normal value. Consequently, reduced crack growth rate effects are closely related to the size and stress distribution of the plastic zone formed by application of overload. The effect of overload will become negligible when the crack advances so far from the point O (say, point D in Figure 11) that the base line stress intensity generates

large strains compared to the strains produced at that point by the overloading. This may explain why for our Ti-V alloys, the overload affected zone is smaller than the calculated overload plastic zone (Table II). Bathias and Vancon[10] have also observed that for their aluminum alloys, the crack length affected by overload is smaller than the measured plastic zone.

The changes in the fractographic features from the pre-overload region to post overload region (Figure 10) may also be explained in terms of the residual compressive stresses and closure. These factors may lower the effective stress intensity range substantially below that of the applied base line stress intensity range. For example, it may be postulated that for the Ti-24V alloy fatigued at a ΔK_b of 30 MPa$\sqrt{m}$, the effect of 100 cycles of 100% overload is to reduce the effective ΔK to below 18 MPa$\sqrt{m}$. This could then be the reason for the change in FCP mode from noncrystallographic at the preoverload region to faceted at the post overload region (Figure 10).

For a given overload ratio, the magnitude of the compressive stresses is smaller for a test specimen with smaller ΔK_b. However, this decrease may be overcompensated by the much slower release of the residual stresses by the application of smaller ΔK_b cycles. Thus, the number of delay cycles is observed to increase with a decrease in ΔK_b, Figures 2,4 and 6.

The Effect of Material Properties: If the delay effect is assumed to be primarily due to the residual compressive stresses,

then it should depend primarily upon two factors which are (1) the magnitude of the compressive stresses and (2) the rate of release of these stresses by the application of post overload base line stress intensity cycles. Even when all the loading and geometrical factors are equal, these two factors may be influenced by some materials' properties. The difference between the overload effects on the two Ti-V alloys (Figures 4-7) may be adequately explained in terms of their monotonic and cyclic deformation behavior and stress-strain response, Figure 12. The Ti-32V alloy has higher monotonic flow stresses, compared to the 24%V alloy. Therefore it is expected to have higher residual stresses in front of the post overload crack tip. However, the Ti-32%V alloy also cyclic softens at low strains. Therefore, it is expected to have a faster rate of release of these stresses, especially at lower baseline stress intensities. As a result of these two opposing factors, the Ti-32V alloy shows smaller N_d values at lower ΔK_b for one cyclic overload.

The Effect of Number of Overload Cycles: The repeated overload cycles leads to changes in the nature of the crack tip in two important ways. One, it alters the residual stresses at the crack tip by cyclic hardening (or softening) of the material. Two, it increases the cyclic damage in the crack tip material. Cyclic hardening will increase the delay cycles whereas the cyclic damage will decrease the delay cycles. Since our results, Figure 4, show a substantial increase in delay cycles with increase in number of overload cycles, it appears that cyclic

hardening is the most important factor. Also, since the cyclic hardening rate of the Ti-24V alloy is much higher than that of the Ti-32V alloy, the difference between the overload effects for one and 100 overload cycles is much larger for the Ti-24V alloy. The Ti-32V alloy fatigue softens only at low strains, and at the stress intensities used during application of the overload cycles fatigue hardening is expected at the crack tip. Therefore, an increase in the delay effect due to an increase in the number of overload cycles is to be expected for this alloy.

The Effect of Overload Ratio: An increase in the overload ratio increases the value of K_{OL} for a given ΔK_b. This increases the magnitude of the compressive residual stresses ahead of the crack tip as well as the overload plastic zone size. As a result a large increase in the number delay cycles is observed, Figure 6 and 8. The number of ΔK_b cycles required to release compressive residual stresses is expected to increase drastically with an increase in the magnitude of the residual stresses and therefore a drastic increase in delay cycles is observed due to an increase in the overload ratio, Figure 8. The difference between the Ti-24V and Ti-32V alloys with respect to the effect of overload ratio on their delay behavior (Figure 6) for 100 overload cycles, may be explained in terms of their cyclic hardening behavior shown in Figure 12. Ti-24V alloy shows a larger difference because it shows a greater degree of cyclic hardening and therefore, the flow stresses of the crack tip

material is much higher after 100 cycles of 100% overload compared to that after 100 cycles of 50% overload. The difference between N_d for the Ti-24V alloy decreases at higher ΔK_b values (Figure 6) because saturation flow stresses are approached for both the 50 pct and 100 pct overload cycles and the differences in the saturation flow stresses are small for this alloy (i.e., the slope of the cyclic stress-strain curve, n', is small).

The Effect of Stress Ratio: Table IIIa shows that there is a large decrease in the number of delay cycles with an increase in stress ratio from 0.1 to 0.5 or 0.67. It is not expected that an increase in stress ratio will decrease the crack tip blunting or crack tip strain hardening effects. Therefore, the results indicate that these factors do not have any substantial contribution to the delay behavior, and residual compressive stresses have the major contribution. A large stress ratio of 0.5 or 0.67 virtually nullifies the effect of these stresses and a drastic reduction in delay cycles is observed. However, since some delay effect is observed even at a stress ratio as high as 0.67, it appears that strain hardening and blunting may have some small contributions.

The results shown in Table IIIb seem to agree with the foregoing explanations. When the number of delay cycles are increased, a large change in delay cycles is observed for a low stress ratio and a small change is observed for a high stress ratio, even though a large crack tip hardening is present due to 100 overload cycles for both cases. This is again because the high stress

ratio leads to a drastic reduction in the effect of compressive residual stresses on ΔK_b cycles.

The results shown in Table IIIc demonstrate that the most important factors for the number of delay cycles, for a given baseline stress intensity range are (1) the stress ratio of ΔK_b and (2) the value of the overload stress intensity (K_{OL}). This again agrees well with our explanations of the delay behavior.

CONCLUSIONS

1. Complete crack arrest and subsequent slow fatigue crack growth have been observed during fatigue cycling of the Ti-V alloys immediately following an application of overload. The number of crack arrest cycles increases with an increase in the overload ratio or the number of overload cycles. For a given overload ratio, an increase in stress ratio of a constant baseline stress intensity range drastically decreases the number of delay cycles. For the given overload ratio, baseline stress intensity range and stress ratio, a change in the overload stress intensity range has a negligible effect on the number of delay cycles. These may be explained in terms of the compressive residual stresses and crack closure effects due to the greater plastic deformation at and around the crack tip during the application of the overload.

2. Fractographic observations show that the cracking mode is substantially changed from pre to post overload region, which demonstrates that the effective stress intensity range may be much

smaller than the applied ΔK_b when the crack tip is in the immediate post overload region.

3. The Ti-24V alloy shows greater retardation behavior in low ΔK_b range and the Ti-32V alloy shows greater retardation behavior in the high ΔK_b range. This has been attributed to the lower monotonic flow stresses and greater cyclic hardening behavior of the Ti-24V alloy.

4. The difference between the retardation effect due to single and multiple overload cycles is greater for the Ti-24V alloy than for the Ti-32V alloy. This has been attributed to the larger cyclic hardening of Ti-24V than Ti-32V, which leads to comparatively higher residual compressive stresses for the Ti-24V alloy.

ACKNOWLEDGMENTS

The authors wish to acknowledge Dr. E. A. Starke, Jr., for his contributions in various phases of this research. This work was supported by the Office of Naval Research under Contract N00014-75-C-0349, Dr. Bruce A. McDonald, Control Monitor.

REFERENCES

1. R. E. Jones, Eng. Frac. Mech., 5, 585, 1973.
2. R. D. Brown, Eng. Frac. Mech., 10, 409, 1978.
3. P. J. Bernard, T. C. Lindley, C. E. Richard, Metal Science, p390, August 1977.
4. R. P. Wei, T. T. Shih, Int. Journal of Fracture, 10, 77, 1974.
5. J. F. Knott, A. C. Pickard, Metal Sci., p399, August 1977.
6. A. E. Gemma, D. E. Allison, S. W. Hopkins, Eng. Frac. Mech., 9, 647, 1977.
7. D. A. Cobly, P. F. Packman, Eng. Frac. Mech., 5, 479, 1973.
8. J. Schijve, D. Brock, P. DeRegle, NLR Report, M2094.
9. Hardrath, A. T. McEvily, Proc. Crack Prop, Symp., Vol. 1, 1961.
10. C. Bathias and M. Vancon, Eng. Frac. Mech., 10, 409, 1978.
11. W. J. Mills, R. W. Hertzberg, Eng. Frac. Mech., 7, 705, 1975.
12. G. J. Petrak, Eng. Frac. Mech., 6, 725, 1974.
13. W. Elber, ASTM Symp. on Fatigue Crack Growth Under Spectrum Loads, 1975.
14. J. P. Hickerson, R. W. Hertzberg, Meta. Trans., 3, 179, 1972.
15. T. Endo and J. Morrow, J. of Materials, 4, 159, 1969.
16. S. B. Chakrabortty, T. K. Mukhopadhyay, E. A. Starke, Jr., Acta Met., 26, 909, 1977.
17. S. B. Chakrabortty, E. A. Starke, Jr., Met. Trans. A, 12A, 1901, 1979.
18. J. A. Carlson, D. A. Koss, Acta. Met., 26, 123, 1978.
19. G. W. Salgat, D. A. Koss, Material Sci. Eng., 35, 265, 1978.
20. H. G. Paris, B. G. LeFevre, E. A. Starke, Jr., Technical Report, Office of Naval Research Contract N00014-75-1-0349, NR-301-750, 1976.

21. Fu-Wen Ling, E. A. Starke, Jr., Met. Trans., 4, 1971, 1973.

22. Fu-Wen Ling, E. A. Starke, Jr., B. G. LeFevre, Met. Trans., 5, 1979, 1974.

23. H. G. Paris, B. G. LeFevre, E. A. Starke, Jr., Met. Trans., 7, 273, 1976.

24. E. E. Underwood and S. B. Chakrabortty, "Quantitative Fractography of a Fatigued Ti-28 wt pct V Alloy", in Fractography and Materials Science, ASTM STP No. 733 (in press).

25. W. G. Clark and S. J. Hudak, Jr., J. Test. Eval., 3, 454 1975.

26. J. Scijve, P. DeRijk, The Effect of Ground-to-Air-Cycle on the Fatigue Crack Propogation in 2024-T3 Alclad Sheet Material, NLR, TRM, 2148, 1966.

27. W. Elber, Eng. Frac. Mech., 2, 37, 1970.

28. J. E. Srawley, On the Sharpness of Crack Compared with Wells' COD, NASA TMX-52904, 1970.

29. T. H. Sanders, R. J. Bucci, A. B. Thakker, R. R. Sawtell, and J. T. Staley, "Ranking 7XXX Aluminum Alloy Fatigue Crack Growth Resistance Under Constant Amplitude and Spectrum Loading," presented at ASTM Committee E-9 Symposium on: Effect of Load Spectrum Variables on Fatigue Crack Growth Initiation and Propagation, San Francisco, 21 May 1979. To be published in ASTM STP.

30. T. K. Mukhopadhyay, Ph.D. Thesis, Georgia Institute of Technology, Atlanta (USA, 1979.

LIST OF TABLES

LIST OF FIGURES

Table I Composition, Heat Treatment, Microstructure and Tensile Deformation Mode of Alloys Used for Overload Studies

Alloy*	Treatment	Microstructure $\lambda^{\ddagger}$, μm	Tensile Deformation Mode
Ti-24V	As-quenched	64	Coarse Twinning + Wavy Slip
Ti-32V	As-quenched	108	Coarse Single Slip

* All alloys contain approximately 0.2% oxygen

‡ λ is the Mean Grain Intercept Length

Table II Comparison Between the Measured Overload Affected Zone Size (OAZ) and the Calculated Overload Plastic Zone Size (OPZ) for the Ti-24V Alloy for A Single Cycle 100% Overload

ΔK MPa	K_{OL} MPa	OAZ mm	OPZ* mm
11	24	.12	0.22
26	57	.60	1.26

* $OPZ = 2r_y = K_{OL}^2/3\pi\sigma_y^2$, $\sigma_y = 520$ MPa

Table III The Effect of Stress Ratio on the Delay Behavior for the Ti-32V Alloy (the load program is shown in Figure 9).

a) ΔK_b= 11 MPa$\sqrt{m}$, ΔK_{OL}= 22 MPa$\sqrt{m}$, N_{OL}= 1

Program	R	N_d
A	0.1	20,000
B	0.5	5,000
C	0.67	4,000

b) ΔK_b= 11 MPa$\sqrt{m}$, ΔK_{OL}= 22 MPa$\sqrt{m}$

Program	R	N_d	
		N_{OL}=1	N_{OL}=100
A	0.1	20,000	60,000
B	0.5	5,000	7,000

c) ΔK_b= 8 MPa$\sqrt{m}$, K_{OL}= 16 MPa$\sqrt{m}$, N_{OL}= 100

Program	N_d
A	1,000,000
B	1,000,000

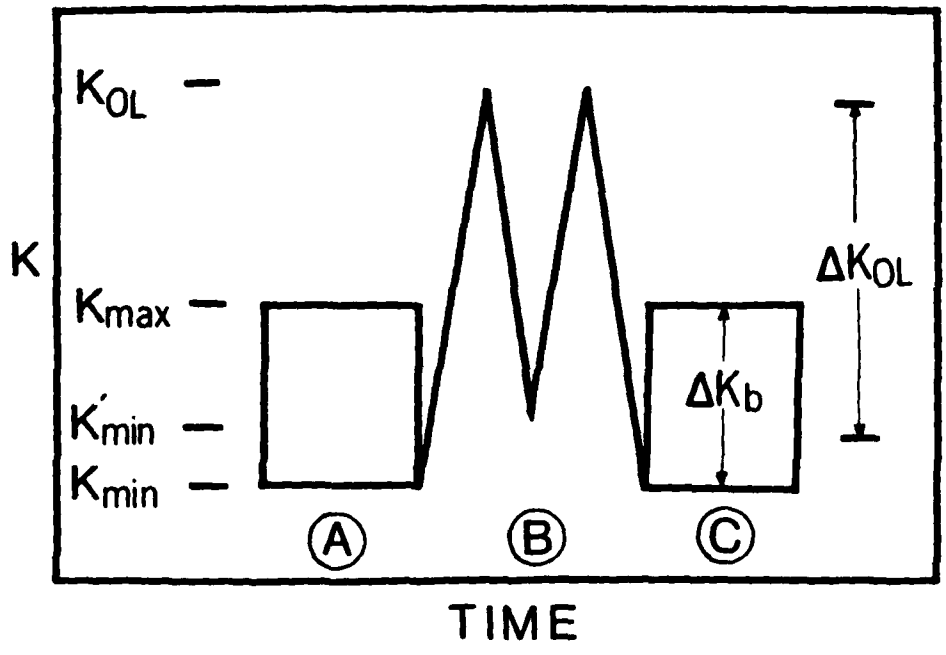

Percent Overload = $100.(K_{OL}-K_{max})/K_{max}$

Overload Ratio, $R_{OL} = K_{OL}/K_{max}$

Stress Ratio, $R = K_{min}/K_{max}$

Figure 1 Schematic Description of a Typical Overload Program.

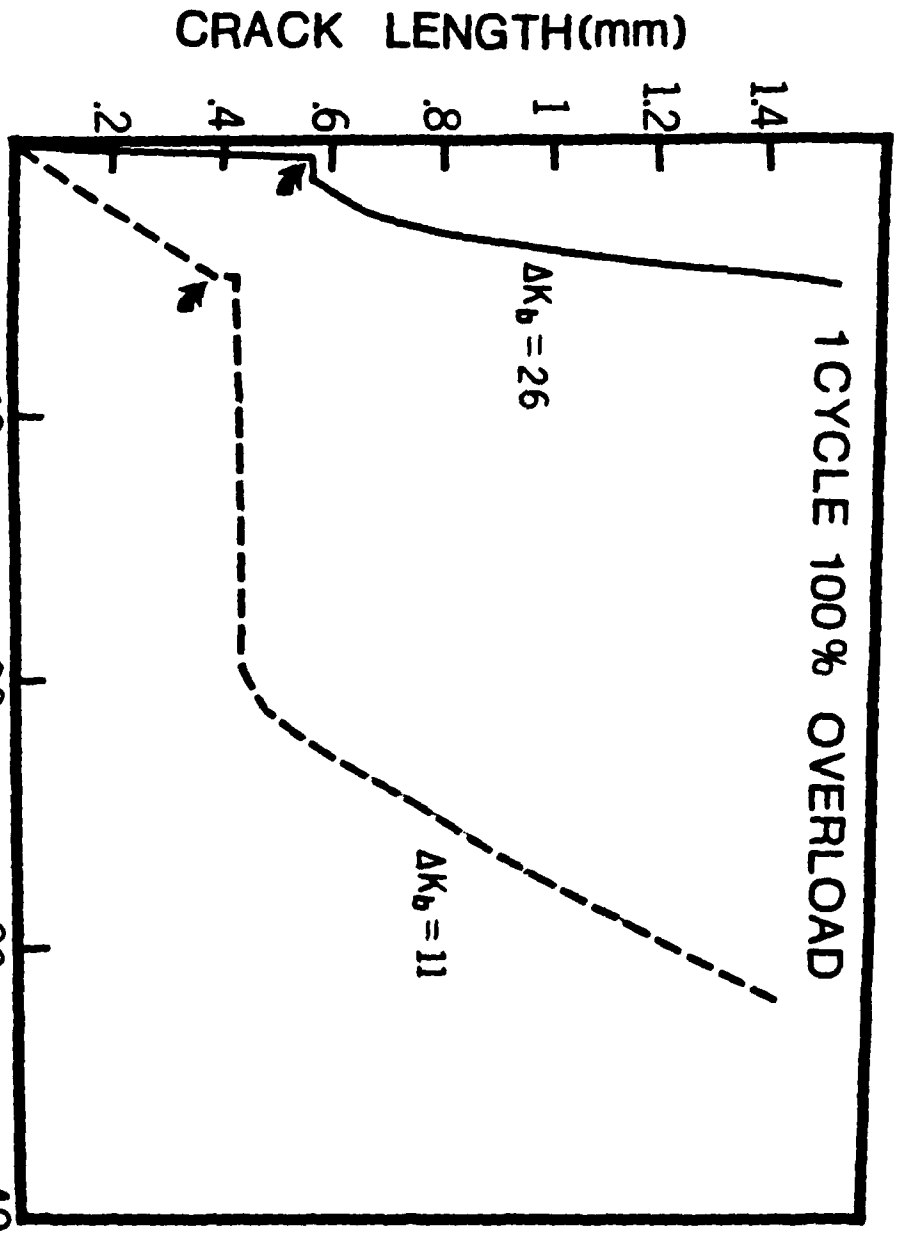

Figure 2 Crack Length versus Number of Cycles, Showing Retardation Behavior of Ti-24V after 1 cycle of 100 pct. Overload.

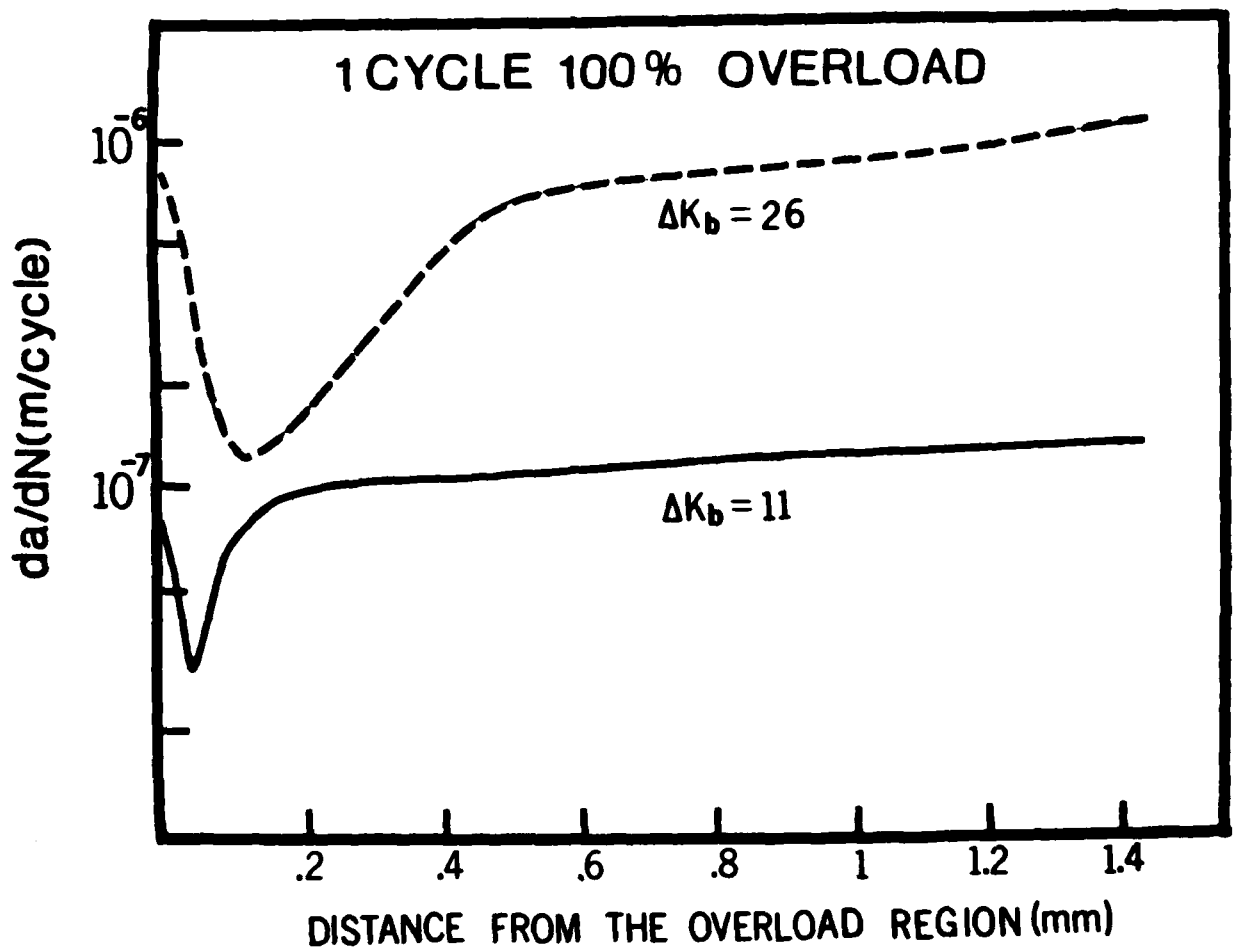

Figure 3 Fatigue Crack Growth Rate versus Distance from the Point of Overloading, Showing Decrease in FCGR of Ti-24V After 1 Cycle of 100 pct. Overload.

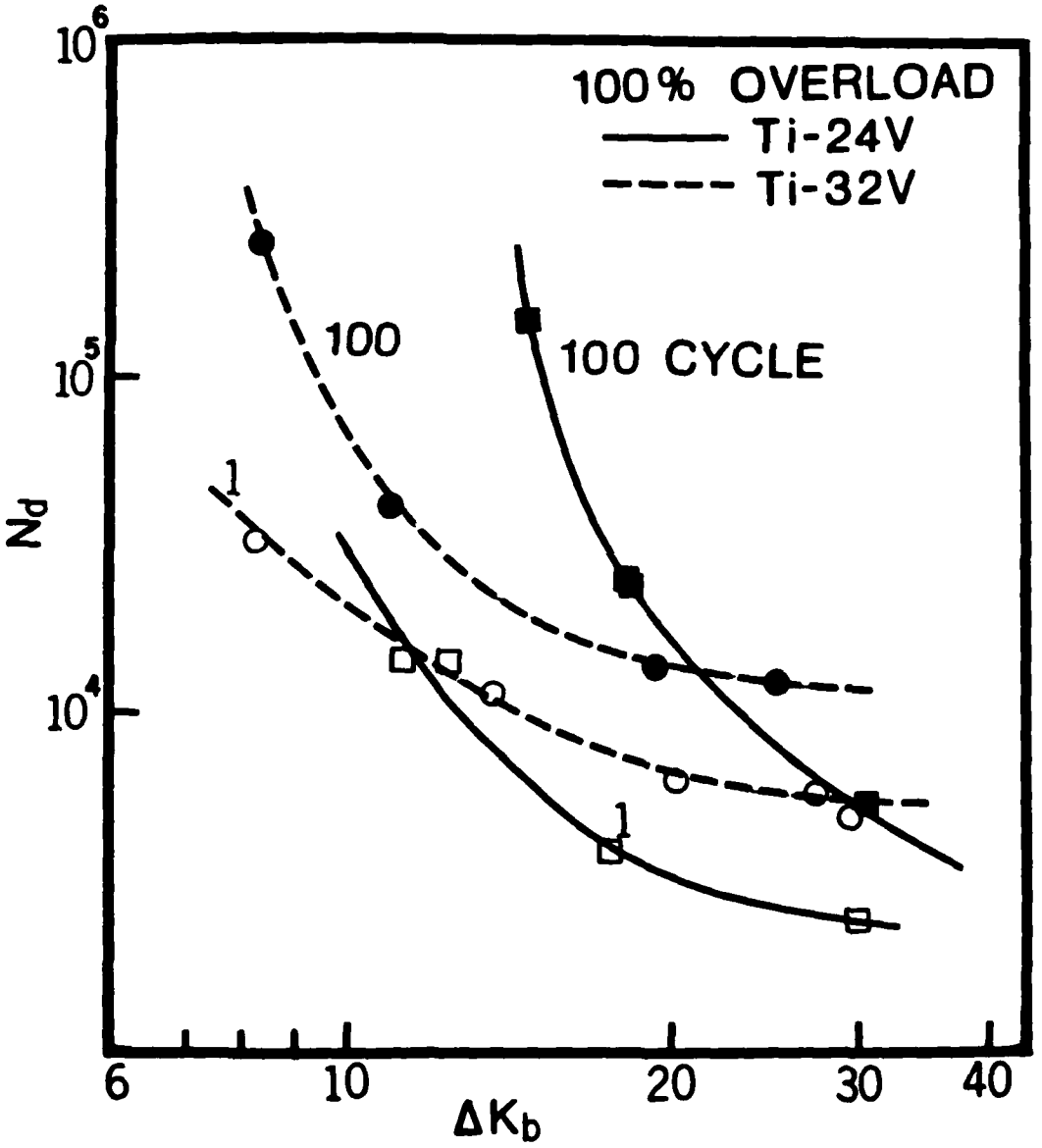

Figure 4 Number of Delay Cycles as a Function of the Base Line Stress Intensity Range for 100 pct. Overload.

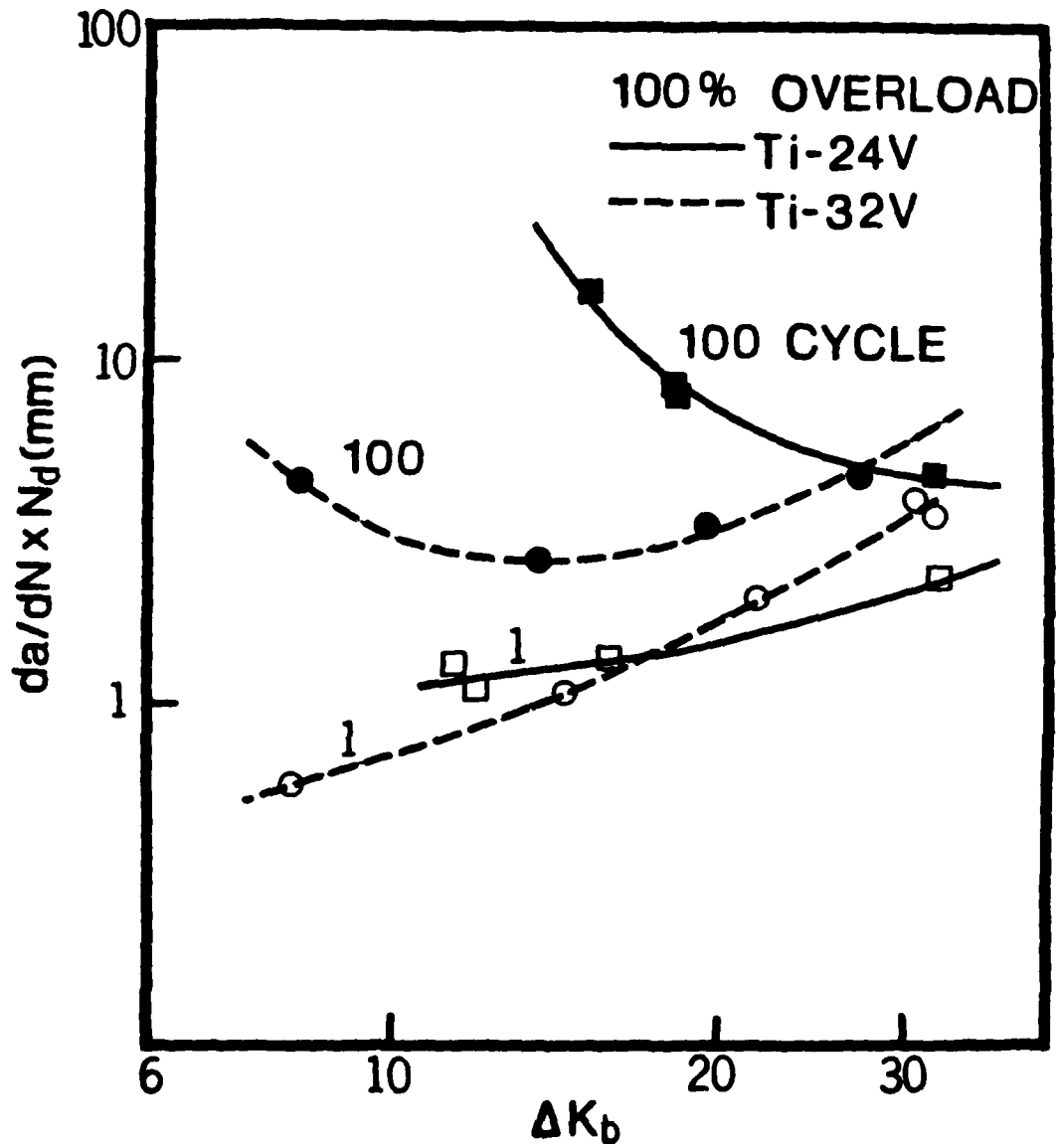

Figure 5 Crack Growth Rate Times the Number of Delay Cycles as a Function of the Base Line Stress Intensity Range for 100 pct. Overload.

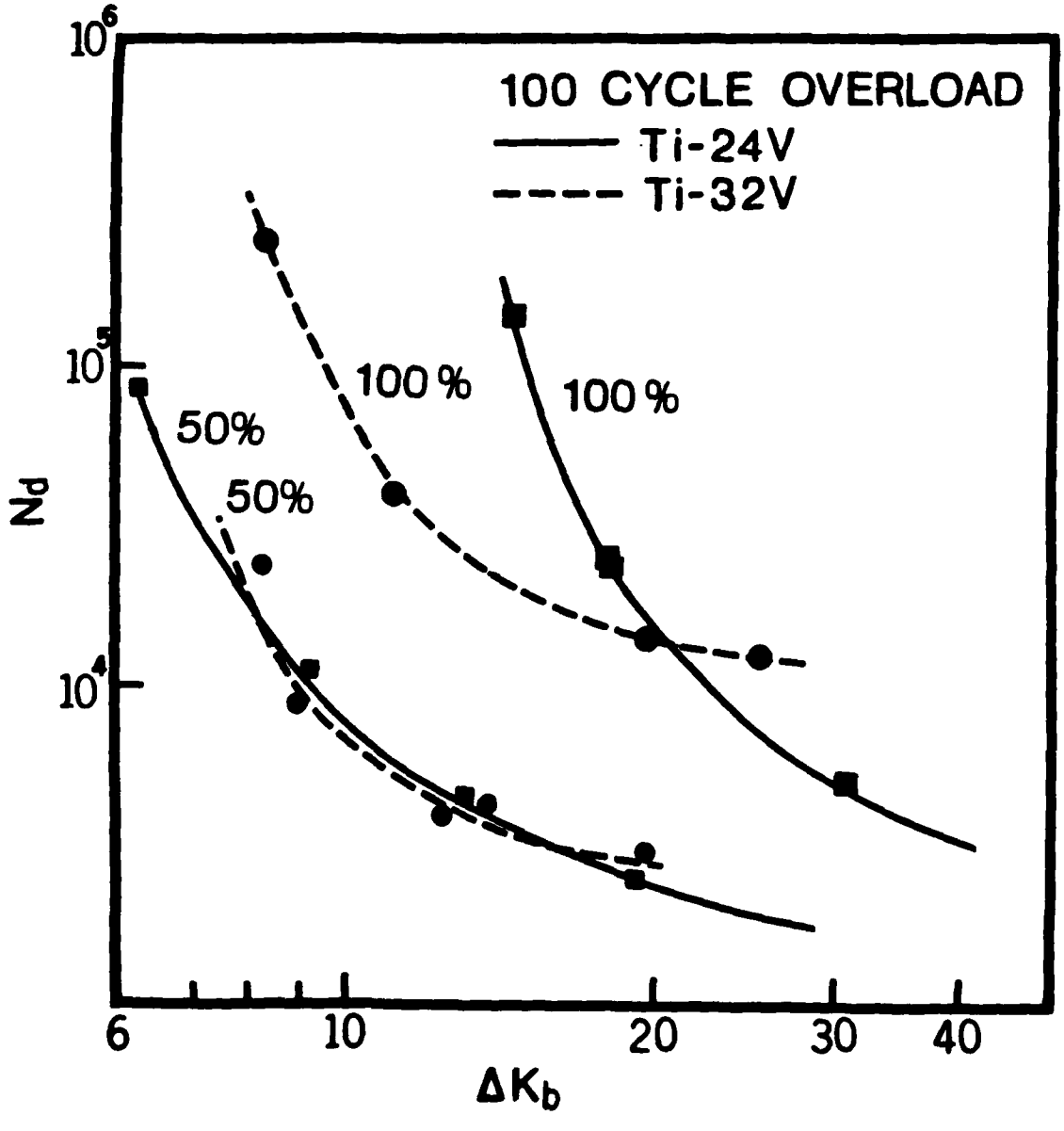

Figure 6 Number of Delay Cycles as a Function of the Base Line Stress Intensity Range for 100 Overload Cycles.

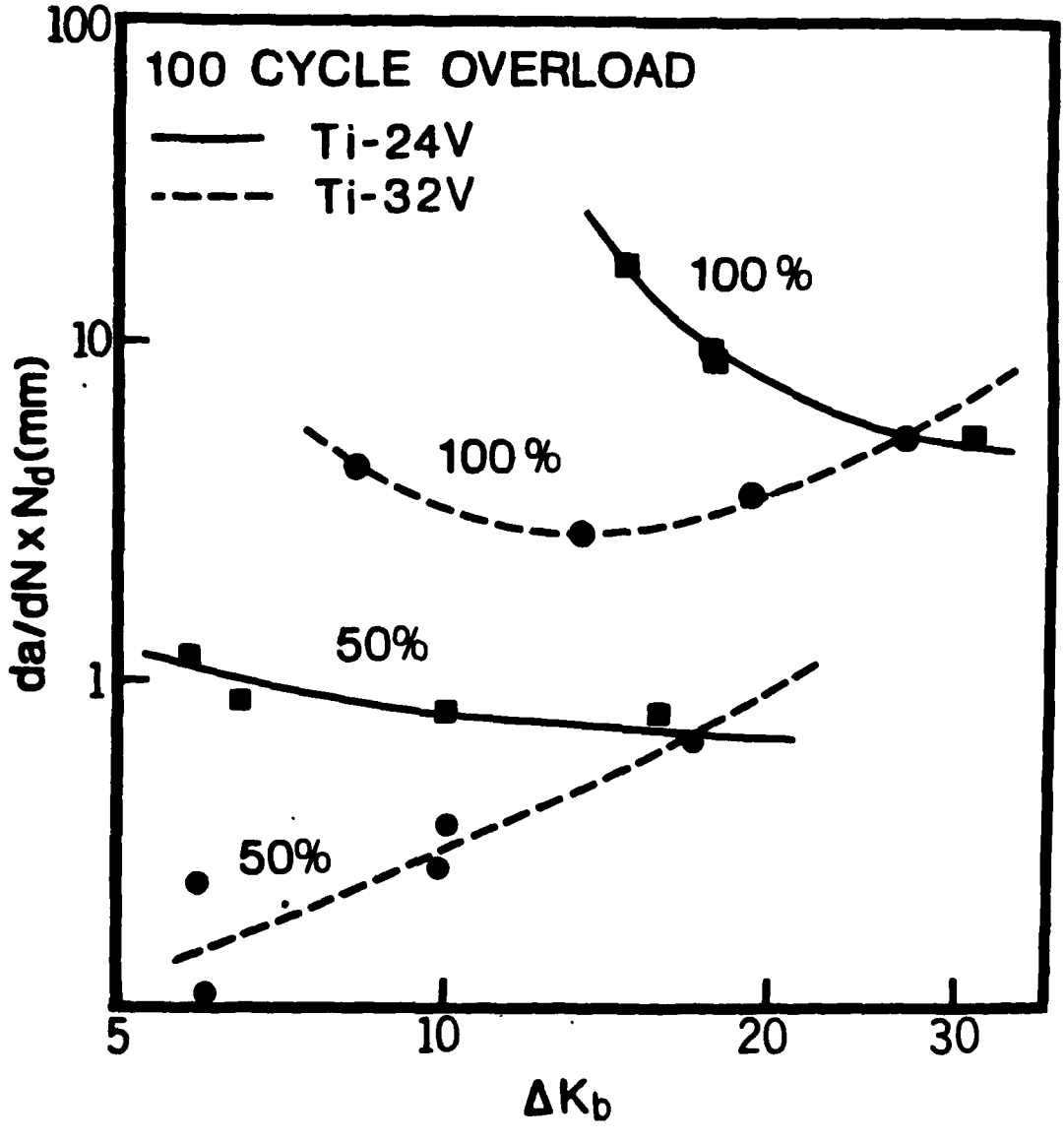

Figure 7 Crack Growth Rate Times the Number of Delay Cycles as a Function of the Base Line Stress Intensity Range for 100 Overload Cycles.

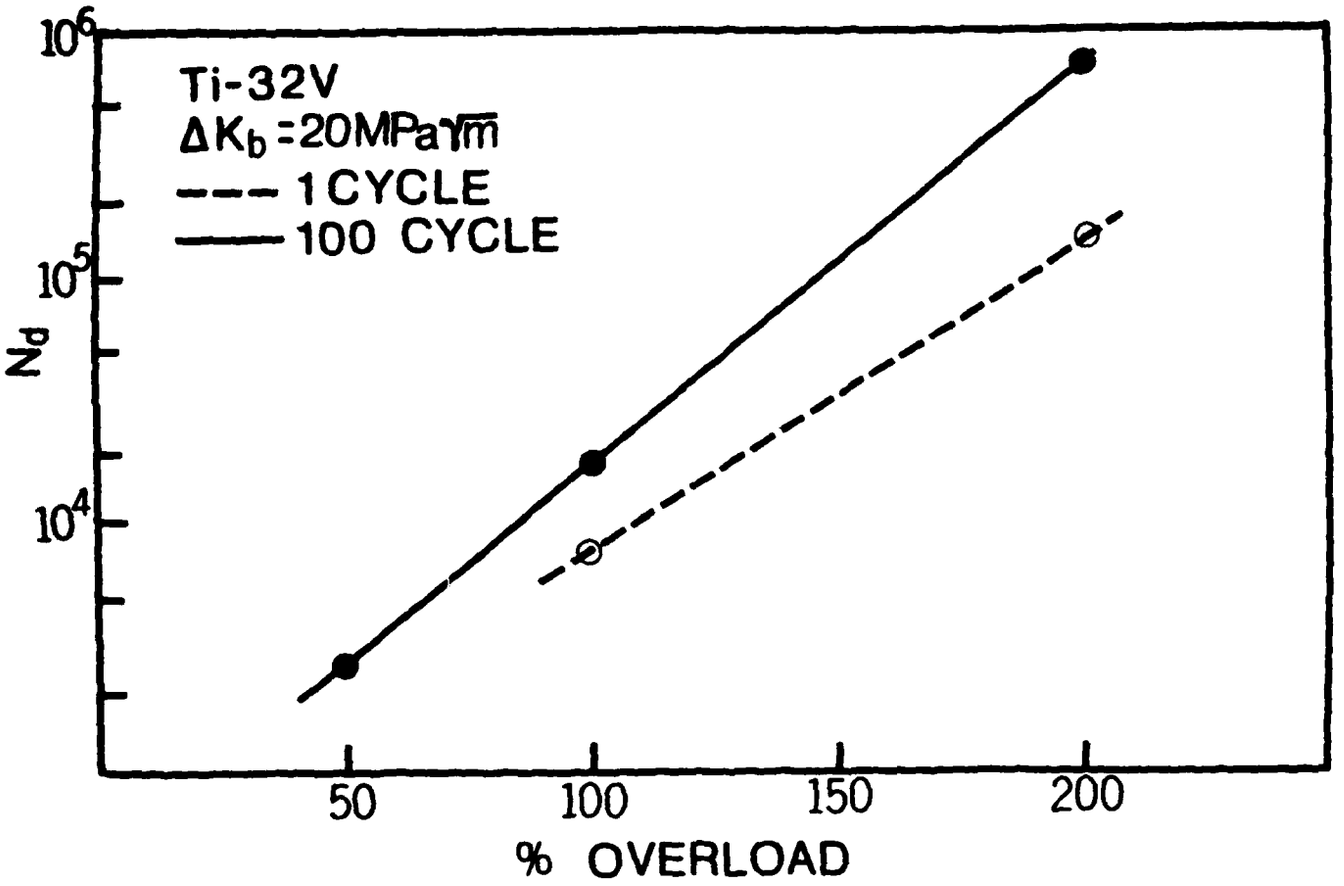

Figure 8 The Effect of Overload Ratio on the Number of Delay Cycles for the Ti-32V Alloy.

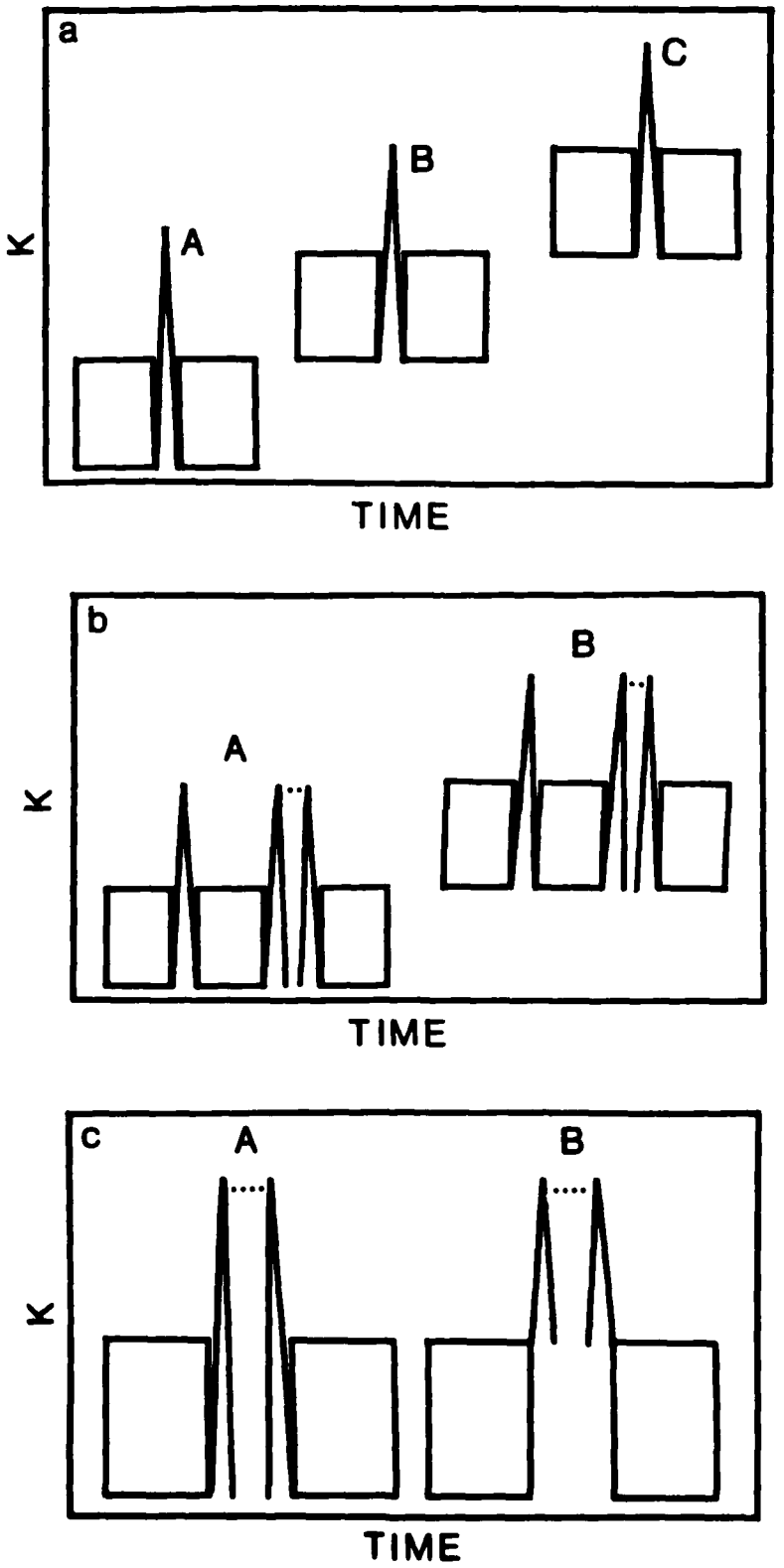

Figure 9 A Schematic of the Load Program used for the Study of the Effect of Stress Ratio on the Delay Behavior for the Ti-32V Alloy.

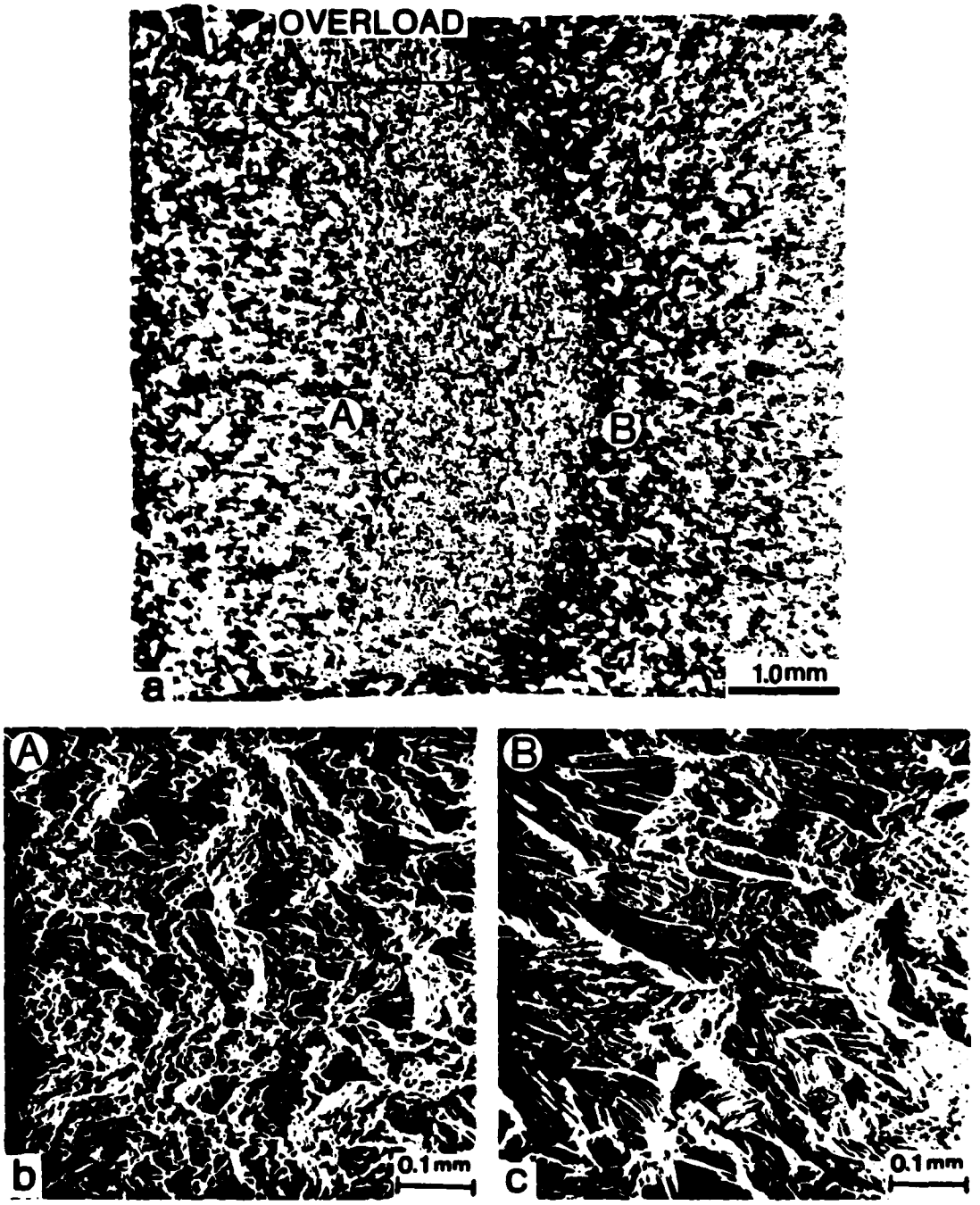

Figure 10 Fracture Surface Features in the Pre and Post Overload Regions of the Ti-24V Alloy for 100 Cycles of 100% Overload at ΔK_b of 30 MPa$\sqrt{m}$.

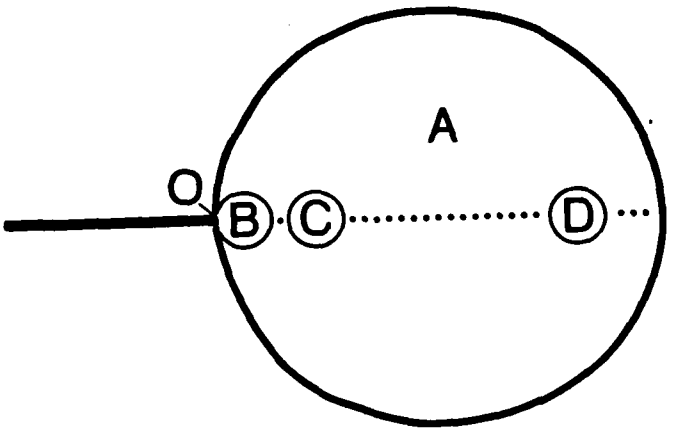

A. Overload Affected Zone

B. Post Overload Zone Where Residual Stress is Reduced During Crack Arrest Cycles.

C. Post Overload Zone Where Residual Stress is Almost Unaffected During Crack Arrest Cycles.

D. Plastic Strain During Overload is Smaller Than That During Post Overload Cycles

O. Crack Tip Position Just After the Application of Overload.

Figure 11 A Schematic of Plastic Zones at the Crack-Tip after Overload.

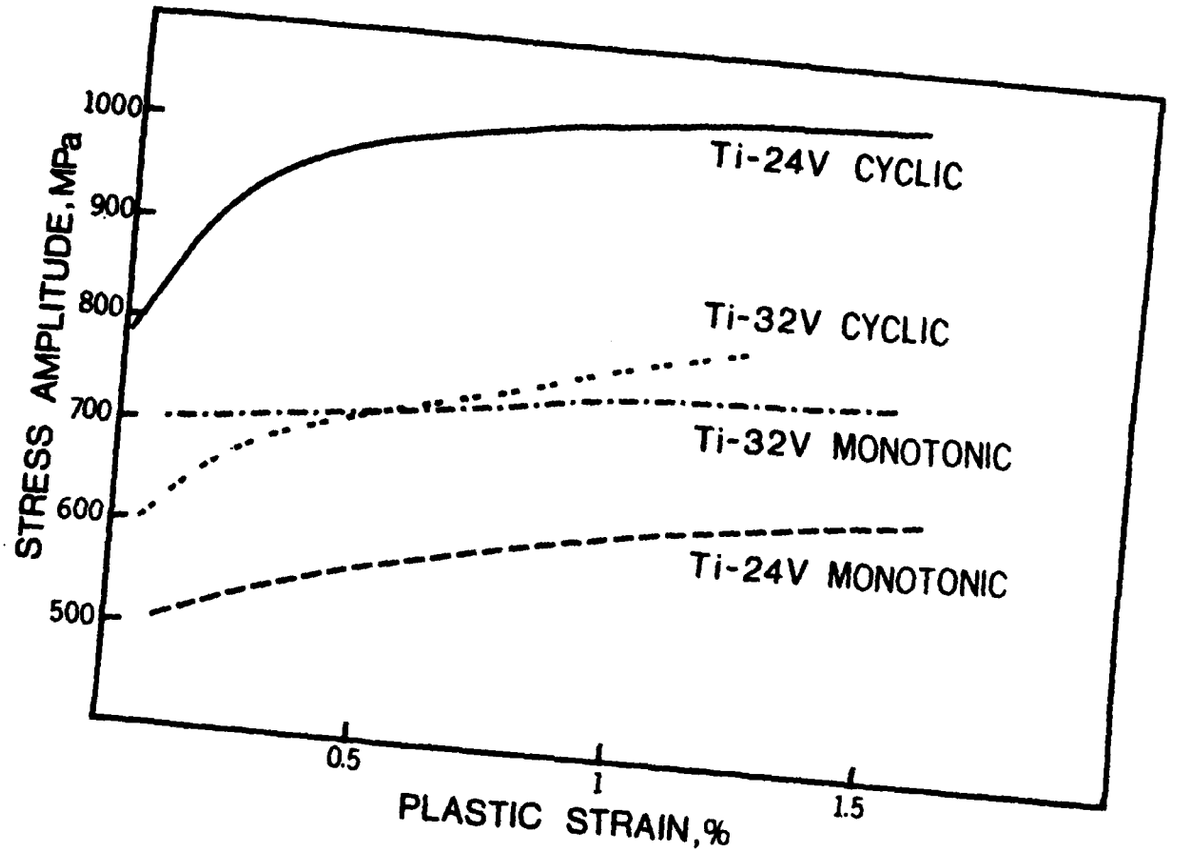

Figure 12 Monotonic and Cyclic Stress-Strain Curves for the Ti-24V and Ti-32V Alloys (Reference 17 and 29).